Arch Appl Mech (2010) 80: 377–388
DOI 10.1007/s00419-009-0320-3

ORIGINAL

Reinaldo Rodríguez-Ramos · Raúl Guinovart-Díaz · Juan C. López-Realpozo · Julián Bravo-Castillero · Federico J. Sabina

Influence of imperfect elastic contact condition on the antiplane effective properties of piezoelectric fibrous composites

Received: 26 September 2008 / Accepted: 25 March 2009 / Published online: 14 April 2009

Abstract A fiber-reinforced periodic piezoelectric composite, where the constituents exhibit transverse isotropic properties, is considered. The fiber cross-section is circular and the periodicity is the same in two orthogonal directions. Imperfect mechanic contact conditions at the interphase between the matrix and fibers are represented in parametric form. In order to analyze the influence of the imperfect interface effect over the behavior of the composite, the effective axial piezoelectric moduli are obtained by means of the Asymptotic Homogenization Method. Some numerical examples are given.

Keywords Asymptotic homogenization · Piezoelectric composites · Linear spring interface model · Imperfect contact

1 Introduction

It is well known that interface imperfections can significantly affect the mechanical properties and failure mechanisms as well as the strength of fibrous composites. The nature of the bond between fibers and the matrix material has a significant effect on the mechanical behavior of fibrous composites. Most analytical and numerical models assume that the bond between the fiber and matrix is perfect and it can be modelled using the continuity of tractions and displacements across a discrete interface. However, internal defects and imperfect interfaces are well known to exist in composites and the incorporation of such phenomena into the general theory requires modification and relaxation of the continuity of displacements between the constituents. The imperfect interface bond may be due to a very compliant thin interfacial layer known as interphase or interface damage. Such an interfacial zone may have also been introduced deliberately by coating the fibers in order to control the mechanical response and fatigue life of the composite. It may also develop during the manufacturing process due to chemical reactions between the contacting fibers and matrix material or due

R. Rodríguez-Ramos (✉) · R. Guinovart-Díaz · J. C. López-Realpozo · J. Bravo-Castillero
Facultad de Matemática y Computación, Universidad de La Habana,
San Lázaro y L, Vedado, 10400 Habana 4, Cuba
E-mail: reinaldo@matcom.uh.cu

R. Rodríguez-Ramos · R. Guinovart-Díaz · J. C. López-Realpozo · J. Bravo-Castillero
Campus Estado de México, División de Arquitectura e Ingeniería,
Instituto Tecnológico de Estudios Superiores de Monterrey,
Apartado Postal 6–3, Atizapán, 52926 Mexico, Mexico

F. J. Sabina
Instituto de Investigaciones en Matemáticas Aplicadas y en Sistemas,
Universidad Nacional Autónoma de México, Apartado Postal 20-726,
Delegación de Álvaro Obregón, 01000 Mexico, DF, Mexico
E-mail: fjs@mym.iimas.unam.mx

to interface damage from cycling thermo-mechanical loading. The strength of the bond at the fiber-matrix interface controls the fatigue life of the composite significantly. By controlling the stress–strain response and ductility of the interface region, it is possible to control overall behavior of the composite.

It should be noted that the study of contact phenomena and the modelling of interfaces between two solids gain special importance in the effective property determination of composite media. For example, a composite containing highly conducting particles in a poorly conducting matrix may have an effective conductivity equal to that of the matrix if the Kapitza contact resistance between the matrix and the particles is sufficiently high. Dually, a composite with weakly conducting particles in a highly conducting matrix will have the effective conductivity of the matrix if there is "superconducting contact" between particles and matrix (the normal heat flux across the interface exhibits a discontinuity which is proportional to the surface Laplacian of the temperature). These effects were identified by Torquato and Rintoul [43], Lipton and Vernescu [26], and Lipton [27]. Finally, it should be mentioned here that interface effects become specially pronounced in composites containing small size particles, since, for a given volume fraction of host particles in a matrix, the smaller the particle size, the larger will be the total contact surface between particles and matrix. In view of the growing interest in nano-scale phenomena, there has been a series of recent contributions in the literature on the effect of interfaces in solids (see, for example [8–10,31,41]).

In Bövik [6], the simple idea of a Taylor expansion of the relevant physical fields in thin regions combined with surface differential operators on a curved surface has been used in achieving the representation of a thin interphase by an interface. The idea of a Taylor expansion was also used in deriving spring-type interface model for soft elastic interphases [18], for highly conducting thin interphases [32], and for interphases of arbitrary conductivity and elastic moduli [19,20]. All of the above studies have assumed that the interphase is isotropic. Niklasson et al. [36,37] have extended the Bövik model to flat anisotropic layers.

Furthermore, several studies show that the interface properties strongly affect the macroscopic behavior of composite materials. In particular in the case of composite frictional materials such as reinforced soil [2,11,35]. Some other approaches by [22,23] for studying composite with imperfect contacts are reported where the effect of an inhomogeneous interphase on the elastic constants is studied.

This work is motivated by the interest to study the influence of non-perfect interfacial contact over the effective piezoelectric response of fibrous composites using the Asymptotic Homogenization Method. It is an extension of the results reported by Sabina et al. [40] and Bravo Castillero et al. [7], where the perfect contact for piezoelectric composites is considered. In this contribution, we have used the same approach that is reported in Molkov and Pobedria (1984) [33], but in this case an extension to piezoelectric composites with elastic imperfect contact condition is considered.

2 Statement of the problem

A two-phase periodic composite is considered here which consists of either a hexagonal or square array of identical parallel circular cylinders embedded in a homogeneous medium. The cylinders are infinitely long (Fig. 1). The material electro-elastic properties of each phase belong to the crystal class 6 mm, where the axes of material and geometric symmetry are both parallel to the x_3 direction. The governing electro-elastic equations for this kind of materials are the Navier equations of linear elasticity and Maxwell's quasistatic equations for the mechanical displacement $\mathbf{u} = (\mathrm{u}, \mathrm{v}, \mathrm{w})$ and electric field $\boldsymbol{E} = (E_1, E_2, E_3)$. They become coupled equations for $\mathbf{u}$ and $\boldsymbol{E}$ through the constitutive relations of the medium. In a two-dimensional situation, like in the considered geometry here, it is well-known that the equations of elasticity (with no piezoelectricity present) for, say, two isotropic solids uncouple into two independent systems under suitable boundary conditions. Namely, the familiar plane- and antiplane-strain deformation states. The in-plane displacement components $u(x_1, x_2)$, $v(x_1, x_2)$ only appear in the former state. In the later one the remaining out-of-plane displacement $w(x_1, x_2)$ is present (see, e.g., [34, p. 82]). A similar situation arises when there is piezoelectric coupling, i.e., for the full electro-elastic equations Benveniste [4] has shown that, under certain loading conditions at the (cylindrical) external boundary of solids of class 2, the electro-elastic equations uncouple also into two separate problems. Although it is not mentioned explicitly there, the same uncoupling occurs for solids of the class 6 mm considered here. One of them, involves u, v, E_3, i.e., it is a state of in-plane mechanical deformation and out-of-plane electric field. The other state, which is of particular interest here, is characterized by an out-of-plane mechanical displacement w and an in-plane electric field of components E_1 and E_2.

The main aim of this paper is the determination of the shear piezoelectric effective properties, denoted by $\bar{p}$ (longitudinal shear modulus), $\bar{s}$ (shear stress piezoelectric coefficient) and $\bar{t}$ (transverse permittivity constant)

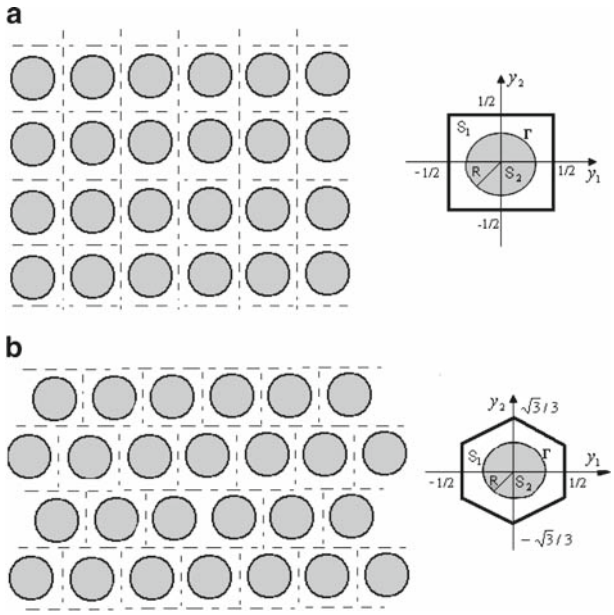

Fig. 1 **a** Square arrangement of fibers and periodic cell. **b** Hexagonal arrangement of fibers and periodic cell. The piezoelectric domains S_1 and S_2 are the matrix and the cylindrical fibers with radius R, respectively, separated by the interface Γ

using the homogenization method as in Bravo Castillero et al. [7]. In that paper the same cylindrical geometry is considered and the phases are solids of the class 6 mm. The above-mentioned uncoupling occurs, but it turns out that the electromechanical variables $u,\ v,\ E_3$ satisfy the same equations as the class 6 mm. It is not so for the other electromechanical state. Thus it is only necessary to solve for the remaining one relating $w,\ E_1,\ E_2$. In this case the relevant constitutive relations are

$$\sigma_{23} = 2p\varepsilon_{23} - sE_2, \quad \sigma_{13} = 2p\varepsilon_{13} - sE_1, \quad D_1 = 2s\varepsilon_{23} + tE_1, \quad D_2 = 2s\varepsilon_{13} + tE_2, \tag{1}$$

where $\sigma_{13},\ \sigma_{23}$ are stress components; $\varepsilon_{13},\ \varepsilon_{23}$ those of strain; $D_1,\ D_2$ in-plane electric displacement components; only three material properties appear here, namely, the longitudinal shear modulus, the transverse permittivity constant and the shear stress piezoelectric coefficient. Note the differential relations $2\varepsilon_{13} = w_{,1}, \quad 2\varepsilon_{23} = w_{,2}, \quad E_1 = -\varphi_{,1}, \quad E_2 = -\varphi_{,2}$, where φ is the associated electric potential and the comma notation is understood to denote differentiation with respect to x_i, i.e., $\varphi_{,1} \equiv \partial\varphi/\partial x_1$.

The equilibrium equations in the composite are

$$\sigma_{13,1} + \sigma_{23,2} = f, \qquad D_{1,1} + D_{2,2} = 0, \tag{2}$$

where f is the body force [21].

The two phases are assumed to have only an imperfect elastic contact along the interface of each cylinder which is denoted by Γ (Fig. 1). Then, the boundary conditions of the imperfect elastic bonding will correspond to the continuity of traction across the interface (the equilibrium conditions of the medium are satisfied) but there exist jumps in the displacement (the continuity conditions are not satisfied so that a certain sliding occurs), i.e., in this case the jumps are in the tangential direction. Moreover, continuity conditions of potential and normal component of electric displacement remain unchanged by this effect. Thus,

$$||\sigma_{13}n_1 + \sigma_{23}n_2|| = 0 \quad \text{on } \Gamma, \tag{3}$$

$$\sigma_{\alpha 3}^{(1)} = \sigma_{\alpha 3}^{(2)} = (Kp^{(1)}/R)(w^{(1)} - w^{(2)}) \quad \text{on } \Gamma, \alpha = 1, 2, \tag{4}$$

$$||\varphi|| = 0 \quad \text{on } \Gamma; \ ||D_1n_1 + D_2n_2|| = 0 \quad \text{on } \Gamma. \tag{5}$$

where $n = (n_1, n_2)$ is the unit normal vector to Γ. The double bar notation is used to denote the jump of the relevant function across Γ taken from the matrix to the fiber. The superscripts 1 and 2 denote the matrix and

fiber, respectively; R is radius of the fiber. The parameter $K \quad (0 \leq K < \infty)$ in (4) summarizes mechanical properties of the interface. It is a spring constant-type material parameter which will be called the interface parameter. It is seen that an infinite value of this parameter implies vanishing of the displacement jump and, therefore, perfect contact interface conditions are described. At the other end, zero value of the parameter implies vanishing of interface tractions and, therefore, debonding of the two adjoining media are modelled. Any finite positive values of the interface parameter define an imperfect interface [17,18]. Equation (4) is usually called a weak interface condition; it was originally proposed by Goland and Reissner [12] and later studied by many authors such as Benveniste and Miloh [3], Molkov and Pobedria [33], Mahiou and Beakou [29], Benveniste and Miloh [5], Hashin [20] and Andrianov et al. [1].

3 Method of solution

Let l be the distance between the centers of two neighbouring cylinders and L the diameter of the composite. Then, when $\varepsilon = l/L$ is a very small number, it is possible to distinguish two spatial scales, one is $\mathbf{x}$, the slow variable, and the other is $\mathbf{y} = \mathbf{x}/\varepsilon$, the fast variable. The boundary value problem (1)–(5) in the composite with imperfect bonding can be solved asymptotically posing the ansatz

$$w(x) = w_0(x, y) + \varepsilon w_1(x, y) + \mathrm{O}(\varepsilon^2), \quad \varphi(x) = \varphi_0(x, y) + \varepsilon \varphi_1(x, y) + \mathrm{O}(\varepsilon^2), \tag{6}$$

and using the method of two scales. The functions $w_0, \varphi_0, w_1, \varphi_1$ are found to satisfy certain differential equations related to the original system in a unit cell (see Fig. 1) with periodic conditions. It is a well-known derivation whose details can be found elsewhere (e.g. [38]) and is omitted here. Of a greater interest are the so-called local (or canonical) problems associated here with the correction terms w_1, φ_1 to the mean variations w_0, φ_0, since they appear in the formulae of the effective properties. There are four of such problems, which are referred as ${}_{13}L$, ${}_{23}L$, and ${}_{2}L$. A pre-index is used to distinguish similar constants and functions such as displacements and potentials, which appear below. Due to the linearity of the Eqs. (1)–(5), the corrections terms w_1, φ_1 can be obtained as a linear combination of some of such displacements and potentials. This, however, will not be done here, since the main objective of this paper is the characterization of the effective properties $\bar{p}$, $\bar{s}$ and $\bar{t}$. There are several alternatives for each property: two for $\bar{p}$ and $\bar{t}$ and four for $\bar{s}$. As a start, one of them is chosen. It requires the solution of a local problem, say, ${}_{13}L$. This means that is necessary to consider, viz.,

$$\bar{p} = p_v + \langle pM_{,1} + sN_{,1} \rangle, \quad \bar{s} = s_v + \langle sM_{,1} - tN_{,1} \rangle, \tag{7}$$

where $M \equiv_{13} M$, $N \equiv_{13} N$ in this section; the subscript v refers to the Voigt average or arithmetic mean of the relevant quantity. For instance, $p_v = p_1 V_1 + p_2 V_2$, etc. and $V_\gamma \quad (\gamma = 1, 2)$ are the area fractions occupied by the matrix or fiber materials respectively, and $V_1 + V_2 = 1$. The displacement M and potential N, which appear in Eq. (7), are the unique solution of the above mentioned local problem, viz.,

$$\Delta M^{(\gamma)} = 0 \quad \text{in } S_\gamma, \quad \Delta N^{(\gamma)} = 0 \quad \text{in } S_\gamma, \quad ||N|| = 0 \quad \text{on } \Gamma, \tag{8}$$

$$\left|\left|(sM_{,1} - tN_{,1})n_1 + (sM_{,2} - tN_{,2})n_2\right|\right| = 0 \quad \text{on } \Gamma, \langle M \rangle = 0, \quad \langle N \rangle = 0, \tag{9}$$

$$\left(p_\gamma M^{(\gamma)}_{,1} + s_\gamma N^{(\gamma)}_{,1}\right) n_1 + \left(p_\gamma M^{(\gamma)}_{,2} + s_\gamma N^{(\gamma)}_{,2}\right) n_2 + p_\gamma n_1 = \pm K p_1 \, ||M|| \, R^{-1}, \gamma = 1, 2. \tag{10}$$

Note that a combination of Eq. (10) is equivalent to the condition

$$\left|\left|\left(pM_{,1} + sN_{,1}\right) n_1 + \left(pM_{,2} + sN_{,2}\right) n_2\right|\right| = -\,||p||\, n_1, \quad \text{on } \Gamma, \tag{11}$$

where Δ is the two-dimensional Laplacian. Thus $M^{(\gamma)}$ and $N^{(\gamma)}$ are sought such that they are doubly periodic harmonic functions of the complex variable $z = y_1 + iy_2$ in the square or hexagonal unit cell $S (= S_1 \cup S_2$ and $S_1 \cap S_2 = \phi)$ of periods $\omega_1 = 1$ and $\omega_2 = e^{i\mu}$ ($\mu = \pi/2$ or $\mu = \pi/3$). When the piezoelectric coefficients s_1, s_2 vanish, there is no electroelastic coupling. Hence the Eqs. (8)–(11) uncouple in two independent sets. Those for $M^{(\gamma)}$ correspond to the antiplane elastic problem ${}_{13}L$ [40]. The remaining equations for $N^{(\gamma)}$ are homogeneous implying either a null potential or the existence of resonances [30] for the dielectric problem. The study of which is beyond the scope of this paper.

Equations (7) are easily transformed to area integrals applying Green's theorem. The doubly periodic boundary conditions on S and the continuity of displacement and potential on Γ leads to

$$p = p_v - ||p|| \int_{\Gamma} M \mathrm{d}y_2 - ||s|| \int_{\Gamma} N \mathrm{d}y_1, \tag{12}$$

$$s = s_v - ||s|| \int_{\Gamma} M \mathrm{d}y_2 + ||t|| \int_{\Gamma} N \mathrm{d}y_1. \tag{13}$$

4 Solution of the local problem ${}_{13}L$

Methods of potential theory are used to solve Eqs. (8)–(11). Doubly periodic harmonic functions are to be found in terms of the following Laurent and Taylor expansions of harmonic functions:

$$M^{(1)}(z) = \mathrm{Re}\left\{-\pi a_1 R z + \sum_{n=1}^{\infty}{}^{o}a_n \left(\frac{R}{z}\right)^n + \sum_{n=1}^{\infty}{}^{o}\sum_{k=1}^{\infty}{}^{o}a_k \eta_{kn} \left(\frac{z}{R}\right)^n\right\}, \quad \text{in } S_1, \tag{14}$$

$$N^{(1)}(z) = \mathrm{Re}\left\{-\pi b_1 R z + \sum_{n=1}^{\infty}{}^{o}b_n \left(\frac{R}{z}\right)^n + \sum_{n=1}^{\infty}{}^{o}\sum_{k=1}^{\infty}{}^{o}b_k \eta_{kn} \left(\frac{z}{R}\right)^n\right\}, \quad \text{in } S_1, \tag{15}$$

$$M^{(2)}(z) = \mathrm{Re}\left\{\sum_{n=1}^{\infty}{}^{o}c_n \left(\frac{z}{R}\right)^n\right\}, \quad \text{in } S_2, \tag{16}$$

$$N^{(2)}(z) = \mathrm{Re}\left\{\sum_{n=1}^{\infty}{}^{o}d_n \left(\frac{z}{R}\right)^n\right\}, \quad \text{in } S_2, \tag{17}$$

where

$$\eta_{kl} = -\frac{(k+l-1)\ !}{(k-1)\ !l\ !} R^{k+l} \sum_{m=-\infty}^{\infty}\sum_{n=-\infty}^{\infty} \frac{1}{(m\omega_1 + n\omega_2)^{k+l}}, \quad m+n \neq 0, \quad k+l > 2,$$

and a_n, b_n, c_n, d_n are real undetermined coefficients; ω_1, ω_2, are the periods of the hexagonal or square array (see Fig. 1). The superscript "o" next to the summation symbol means that "n" runs only over odd integers so that each term in Eqs. (14)–(17) has the same anti-symmetry property as $M^{(\gamma)}$ and $N^{(\gamma)}$, namely, $M^{(\gamma)}(-z) = -M^{(\gamma)}(z)$, $N^{(\gamma)}(-z) = -N^{(\gamma)}(z)$ [7,13,40].

The line integrals in Eqs. (12)–(13) and the assumed expansions (14)–(17) produce a very simple result as a consequence of the orthogonality of the trigonometric functions, namely,

$$\int_{\Gamma} M^{(1)} \mathrm{d}y_2 = \pi R\left(-V_2 a_1 + a_1 + \sum_{k=1}^{\infty}{}^{o}a_k \eta_{k1}\right), \tag{18}$$

$$\int_{\Gamma} N^{(1)} \mathrm{d}y_2 = \pi R\left(-V_2 b_1 + b_1 + \sum_{k=1}^{\infty}{}^{o}b_k \eta_{k1}\right), \tag{19}$$

$$\int_{\Gamma} M^{(2)} \mathrm{d}y_2 = \pi R c_1, \qquad \int_{\Gamma} N^{(2)} \mathrm{d}y_2 = \pi R d_1. \tag{20}$$

Using Eqs. (14)–(17) the expression (11) can be written in the following form,

$$\left(-p_1 V_2 a_1 - s_1 V_2 b_1 + R\left|\left|p_\gamma\right|\right|\right)\delta_{1n} + p_1\left(\sum_{k=1}^{\infty} {}^{o}a_k \eta_{kn} - a_n\right) + s_1\left(\sum_{k=1}^{\infty} {}^{o}b_k \eta_{kn} - b_n\right) = p_2 c_n. + s_2 d_n, \tag{21}$$

Replacing Eqs. (18)–(21) into Eqs. (12)–(13), we obtain,

$$\bar{p} = p_1 - 2\pi R\,(p_1 a_1 + s_1 b_1), \tag{22}$$

$$\bar{s} = s_1 - 2\pi R\,(s_1 a_1 - t_1 b_1). \tag{23}$$

in which only the residue of $M^{(1)}$ and $N^{(1)}$ contributes towards $\bar{p}$ and $\bar{s}$. The expressions for $\bar{p}$ and $\bar{s}$ in Eqs. (22)–(23) are the same as in the piezoelectric case with perfect contact conditions [7,40]. The coefficients a_1 and b_1, however, are different in both cases. Thus, expressions for a_1, b_1 are now sought from the system of infinite equations

$$MD = U, \tag{24}$$

where the infinite order matrix $M(m_{nk})$, have block components of order two given by

$$m_{nk} = \begin{pmatrix} \delta_{nk} - V_2\beta_1\delta_{1n} + \beta_n\eta_{kn} & \alpha_n^{+}\delta_{nk} - V_2\alpha_1^{-}\delta_{1n} + \alpha_n^{-}\eta_{kn} \\ \delta_{nk} - V_2\gamma_1\delta_{1n} + \gamma_n\eta_{kn} & \delta_n^{+}\delta_{nk} - V_2\delta_1^{-}\delta_{1n} + \delta_n^{-}\eta_{kn} \end{pmatrix}, \tag{25}$$

$D^T = (a_1, b_1, a_3, b_3, \ldots)$, and $U^T = -R\,(\beta_1, \gamma_1, 0, 0, \ldots)$. The super index T denotes transpose and the magnitudes $\alpha_n^{\pm}$, β_n, γ_n, $\delta_n^{\pm}$ are given as follows,

$$\beta_n = \left(\chi^* K - n\chi^* - K\right)/\left(\chi^* K + n\chi^* + K\right), \quad \alpha_n^{\pm} = (s_1/p_1)\left(s^* K \pm n\chi^* \pm K\right)/\left(\chi^* K + n\chi^* + K\right),$$
$$\gamma_n = \left(s^* K - n s^* - K\right)/\left(s^* K + n s^* + K\right), \qquad \chi^* = p_2/p_1, \qquad s^* = s_2/s_1 \quad \text{and} \quad t^* = t_2/t_1,$$

$$\delta_n^{\pm} = (t_1/s_1)\left(\pm s_1^2 n s^*/p_1 t_1 - t^+ K \mp K\right)/\left(s^+ K + n s^+ + K\right). \tag{26}$$

The limit case of perfect contact condition for piezoelectric antiplane problem is derived as a particular case of Eqs. (24)–(26) as $K \to \infty$. In this case, the parameters a_1, b_1 are the same that in Sabina et al. [40] (see formula (3.25), p. 1475). The infinite system (24)–(25) is solved by truncation to order N. The numerical results converge quite quickly for low values of N. The truncation order, however, increases as the parameters K, χ^* and the fiber volume fraction have high values. In the numerical examples presented in Sect. 6, the results are given for $N = 10$, because this achieves the require accuracy for the parameters used.

5 Solution of the local problem ${}_1L$

The displacement $M^{(\gamma)}$ and potential $N^{(\gamma)}(\gamma = 1, 2)$ are the unique solution of the local problem ${}_1L$ given by

$$\Delta M^{(\gamma)} = 0 \quad \text{in } S_\gamma, \quad \Delta N^{(\gamma)} = 0 \quad \text{in } S_\gamma, \quad ||N|| = 0, \quad \text{on } \Gamma, \tag{27}$$

$$\left|\left|(sM_{,1} - tN_{,1})n_1 + (sM_{,2} - tN_{,2})n_2\right|\right| = ||t||\,n_1 \quad \text{on } \Gamma, \langle M\rangle = 0, \quad \langle N\rangle = 0, \tag{28}$$

$$\left(p_\gamma M_{,1}^{(\gamma)} + s_\gamma N_{,1}^{(\gamma)}\right)n_1 + \left(p_\gamma M_{,2}^{(\gamma)} + s_\gamma N_{,2}^{(\gamma)}\right)n_2 + s_\gamma n_1 = \pm K p_1\,||N||\,R^{-1}, \tag{29}$$

a combination of Eq. (29) is equivalent to the condition

$$\left|\left|(pM_{,1} + sN_{,1})n_1 + (pM_{,2} + sN_{,2})n_2\right|\right| = ||s||\,n_1, \quad \text{on } \Gamma, \tag{30}$$

The doubly periodic harmonic functions $M^{(\gamma)}$ and $N^{(\gamma)}$ are sought in the form of a series with undetermined real coefficients a_n, b_n, c_n and d_n, like Eqs. (14)–(17).

The effective properties of the composite $\bar{s}$, $\bar{t}$ have the following analytical expressions

$$\bar{s} = s_1 - 2\pi R\,(p_1 a_1 - s_1 b_1), \tag{31}$$

$$\bar{t} = t_1 + 2\pi R\,(s_1 a_1 - t_1 b_1), \tag{32}$$

The unknown constants a_1 and b_1 in this case can be found by solving the systems (24)–(25) except that U^T is replaced by $U^T = -R\left(\alpha_1^-, \delta_1^-, 0, 0, \ldots\right)$. A similar expression is obtained for the effective coefficients in López-López et al. [28].

6 Analysis of results

In many real fiber-reinforced composites, the fiber-matrix adhesion is imperfect: the continuity conditions for stresses and displacements are not satisfied. Linear spring interface model (present model) and interphase models are often used to simulate the interface behaviour of reinforced composite materials. The aim of this section is to point out the effects of the fiber-matrix interface on the piezoelectric properties of composite materials based on the asymptotic homogenization. To date, to the author's knowledge, the problems associated to the calculations of effective properties with piezoelectric materials and inhomogeneities with imperfect interface conditions have not been proposed sufficiently in the literature. Some numerical results, derived from the present model, are given in order to illustrate the effect of the imperfectness of the interface. In the context of the present study, variations of the stiffness of the spring from a full debonding to a perfect bonding interface are considered. There are certain scenarios associated with the full debonding interfaces, for which the cylindrical inhomogeneity becomes equivalent to a hole.

6.1 Elastic case

A unidirectional composite consisting of T300 fibers and epoxy matrix is studied. Constituent properties used are given in Hashin [16]. Figure 2 shows the variation of the normalized axial shear elastic modulus with interface parameter using four different approaches, i.e. AHM recursive [14], AHM three phase exact model [15], GSCS model [16] and the present model, but only for the purely elastic case and square cells. It is seen that there is a significant effect of the imperfection and that measurement of this modulus can be used as an

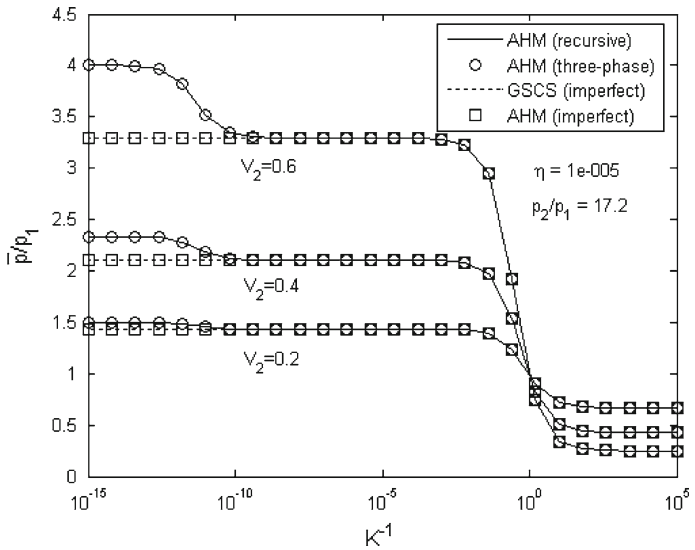

Fig. 2 Effect of elastic interface imperfection on axial shear coefficient for a composite of T300 fibers and epoxy matrix. Comparison of elastic effective modulus $\bar{p}/p_1$ with other models

Table 1 Numerical limit case comparison: perfect contact ($K = 10^{15}$) with imperfect contact condition for the composite of Barium Titanate (matrix) and PZT − 7*A* (fibers)

V_2	$\bar{p}$	$\bar{s}({}_{13}L,\ {}_{1}L)$	$\bar{t}$
0.	29.41	10.6	8.23
0.1	30.6364	10.7229	8.6113
0.2	31.9062	10.8392	9.00741
0.3	33.222	10.9478	9.41924
0.4	34.5865	11.0471	9.84798
0.5	36.0037	11.1346	10.2951
0.6	37.4784	11.2071	10.7626
0.7	39.0168	11.2599	11.253
0.78	40.2985	11.2827	11.6641

experimental means to obtain the interface parameter $K = (p_I/p_1)/\eta$, where p_I is the axial shear modulus of interphase, $\eta = t/R$ and t is the thickness of the interface. Good agreement between all the approaches can be observed. According to the theory of Hashin [20], the connections between a thin interphase model and an interface model can be established by Taylor expansions. In this work, Hashin only studied the connection for elastic fiber-reinforced composites. Recently, the relations between the thin interphase model and interface models were studied for spherical particle-reinforced composites by Wang et al. [44]. Relations between the equivalent interface moduli and the interphase stiffness and thickness were presented by Wang et al. [44]. The AHM (imperfect) model and GSCS (imperfect) are close to each other for a thin thickness of the interphase. Perfect interface is achieved as $K \to \infty$ and debond can be observed as $K \to 0$. Observe that on the left hand side of Fig. 2, the models are separated with respect to AHM (imperfect) since the AHM (three-phase), GSCS (imperfect) and AHM (recursive) models involve three constituents in the composite, whereas the present model for imperfect contact is related to two-phase composite. Obviously, this gap increases, when the volume fraction of the intermediate phase increases. Conversely, the four models are very close on the right-hand side of Fig. 2. Indeed, the above mentioned models are related to imperfect contact.

6.2 Limit cases

The effective elastic modulus $\bar{p}$ is the same that the reported in Molkov and Pobedria [33] for different values of spring constant K. In Table 1 the limit case is studied of perfect contact. The numerical values derived from the analytic expressions reported in Sabina [40] and Bravo Castillero et al. [7] for perfect contact and the present model with square cell for imperfect contact coincide for the effective properties $\bar{p}$, $\bar{s}$ and $\bar{t}$ when the stiffness value of K is very high, for example, $K = 10^{15}$. The effective piezoelectric coefficient $\bar{s}$ [see formulae (23) and (31)] is computed by two different local problems ${}_{13}L$ and ${}_{1}L$. The central column indicates that they are the same. It allows to confirm that the implementation of the numerical code is correct.

Besides, numerical comparisons between the limit case for perfect contact at the interface ($K = 10^{12}$) and complete separation between fibers and matrix ($K = 10^{-12}$) using AHM with square cell and the Generalized Self-Consistent Approach (GSCA) reported by Jiang and Cheung [24] is shown in Table 2. Notice that there is very good agreement between the results using the present model for complete separation and perfect contact and Tables 2 and 3, respectively, reported by Jiang and Cheung [24].

6.3 Overall piezoelectric properties for different arrangements

In Table 3, the matrix is PZT-7A taken from [25] ($p_1 = 29.41$ GPa, $s_1 = 10.60$ C/m^2, $t_1 = 8.23 \times 10^{-9}$ nC/Vm). The piezoelectric effective properties $\bar{p}$, $\bar{s}$ and $\bar{t}$ for different geometric arrays (square and hexagonal cells) of the composite with imperfect contact conditions are illustrated. The ratio of the material properties used are $s_2/s_1 = 6$, $t_2/t_1 = 6$, and the volume fraction is $V_2 = 0.65$.

Different ratios of the axial elastic moduli of the constituents and values of the imperfect parameter K are considered. The parameter K affects the behavior of the elastic, piezoelectric and dielectric properties in the composite. Notice that the values of the effective properties $\bar{p}$, $\bar{s}$ gradually increase whereas $\bar{t}$ decreases when the parameter K increases for each ratio of p_2/p_1. The effective parameters $\bar{s}$ and $\bar{t}$ do not change as $K \to \infty$ since the ratios s_2/s_1 and t_2/t_1 are fixed.

Table 2 Comparison between the limit cases: (**a**) perfect interface ($K = 10^{12}$) and (**b**) complete separation between fiber and matrix ($K = 10^{-12}$) using AHM and the Generalized Self-Consistent Approach (GSCA) reported by Jiang and Cheung [24] in Tables 2 and 3, respectively

Vol. fract.	$\bar{p}$ (AHM)	$\bar{p}$ (GSCA)	$\bar{s}$ (AHM)	$\bar{s}$ (GSCA)	$\bar{t}$ (AHM)	$\bar{t}$ (GSCA)
(a)						
0	21.1	21.000	12.3	12.300	8.107	8.1070
0.1	17.472	17.473	10.064	10.064	6.6592	6.6592
0.2	14.418	14.419	8.2007	8.2007	5.4488	5.4488
0.3	11.812	11.812	6.6238	6.6238	4.4217	4.4217
0.5	7.5992	7.5992	4.1006	4.1006	2.7731	2.7731
0.6	5.8726	5.8726	3.0755	3.0755	2.1014	2.1014
0.8	2.9754	2.9754	1.3669	1.3669	0.97945	0.9794
0.9	1.7482	1.7482	0.64747	0.6475	0.50614	0.5061
(b)						
0	21.1	21.100	12.3	12.300	8.107	8.1070
0.1	17.264	17.264	10.064	10.064	6.633	6.6359
0.2	14.067	14.067	8.2	8.2000	5.4047	5.4096
0.3	11.362	11.362	6.6231	6.6231	4.3653	4.3716
0.5	7.0333	7.0333	4.1	4.1000	2.7023	2.7102
0.6	5.275	5.2750	3.075	3.0750	2.0267	2.0350
0.8	2.3444	2.3445	1.3667	1.3667	0.90078	0.9095
0.9	1.1105	1.1105	0.64737	0.6474	0.42668	0.4355

Table 3 Piezoelectric effective properties $\bar{p}, \bar{s}$ and $\bar{t}$ of the composite of Barium Titanate (matrix) and PZT $-$ 7A (fibers) for different geometric arrays (square and hexagonal) with imperfect contact condition

$V_2 = 0.65$	K	$\bar{p}/p_1$		$\bar{s}/s_1$		$\bar{t}/t_1$	
		Sqr	Hex	Sqr	Hex	Sqr	Hex
$\frac{p_2}{p_1} = 0.1$	0.1	0.2461	0.2903	0.4906	0.4260	11.296	6.9304
	1	0.6864	0.7228	1.9671	1.5061	8.5993	5.6625
	20	1.1167	1.2520	3.4680	2.8432	5.2853	4.0441
	400	1.1575	1.3085	3.6113	2.9888	4.8843	3.8585
	10^{10}	1.1597	1.3116	3.6191	2.9969	4.8613	3.8480
$\frac{p_2}{p_1} = 1$	0.1	0.2487	0.2920	0.3910	0.3803	9.2906	6.3394
	1	0.7669	0.7843	1.6246	1.3446	7.7992	5.4563
	20	1.4480	1.5420	3.4182	2.8514	5.2765	4.0435
	400	1.5298	1.6374	3.6571	3.0460	4.8814	3.8539
	10^{10}	1.5345	1.6429	3.6709	3.0572	4.8578	3.8429
$\frac{p_2}{p_1} = 20$	0.1	0.2532	0.2957	0.2345	0.2816	6.2289	5.0708
	1	0.9711	0.9716	0.8233	0.8581	6.0028	4.8424
	20	3.8361	3.3831	3.0061	2.8978	5.2232	4.0410
	400	5.3345	4.0614	4.0918	3.4657	4.8570	3.8200
	10^{10}	5.4654	4.1069	4.1858	3.5037	4.8256	3.8053
$\frac{p_2}{p_1} = 400$	0.1	0.2538	0.2962	0.2145	0.2661	5.8531	4.8717
	1	1.0089	1.0112	0.6858	0.7562	5.7081	4.7151
	20	5.1746	4.2390	2.7575	2.9176	5.1966	4.0402
	400	9.2320	5.4429	4.5212	3.7040	4.8346	3.8009
	10^{10}	9.7189	5.5307	4.7292	3.7610	4.7931	3.7837
$\frac{p_2}{p_1} = 10^{10}$	0.1	0.2539	0.2963	0.2134	0.2651	5.8318	4.8601
	1	1.0111	1.0136	0.6777	0.7499	5.6907	4.7074
	20	5.2824	4.3032	2.7372	2.9191	5.1945	4.0402
	400	9.6531	5.5548	4.5673	3.7233	4.8322	3.7994
	10^{10}	10.193	5.6466	4.7896	3.7819	4.7896	3.7819

6.4 Effective properties versus fiber volume fraction for different parameter K

In Fig. 3 the electro-elastic effective properties $\bar{p}, \bar{s}, \bar{t}$ and $\bar{d}$ versus fiber volume fraction are shown for the composite Barium Titanate (fiber) ($p_2 = 43.86$ GPa, $s_2 = 11.40$ C/m^2, $t_2 = 12.80 \times 10^{-9}$ nC/Vm) and PZT-7A (matrix) with different values of imperfect parameter K using square cell. The fixed ratio used is $\chi^* = p_2/p_1 = 1.5$. The effective properties are for non-perfect contact approached to the effective properties with perfect contact ($K = 10^{10}$) if the parameter K increases. It was reported by Hashin [17,18].

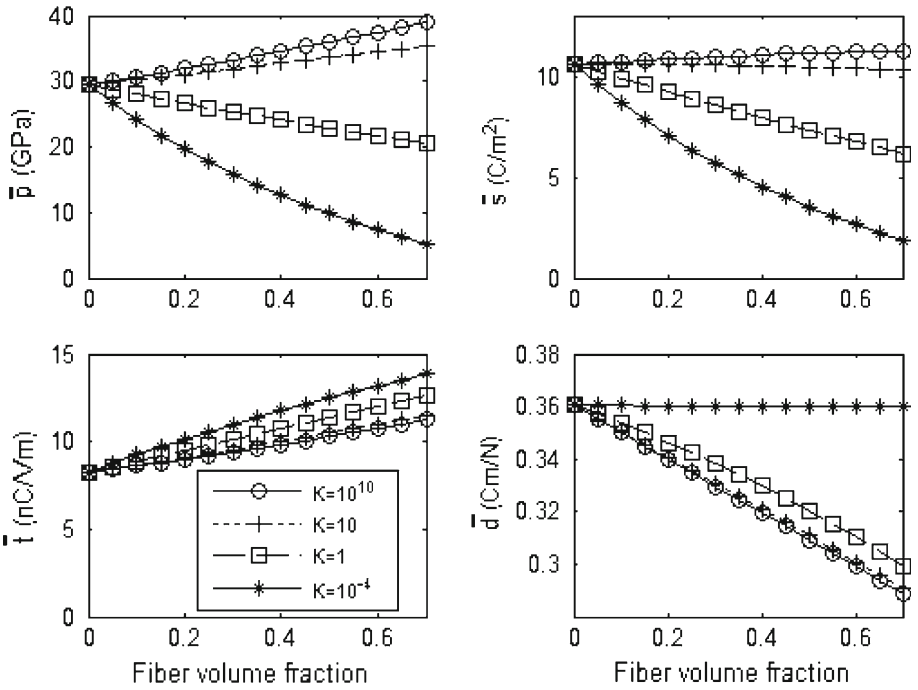

Fig. 3 Electro-elastic effective properties $\bar{p}, \bar{s}, \bar{t}$ and $\bar{d}$ versus fiber volume fraction for a composite of Barium Titanate (matrix) and PZT-7A (fiber) for different values of imperfect parameter K

6.5 Piezoelectric effective properties versus Continuous parameter K for different ratios of $\chi^* = p_2/p_1$

Figure 4 shows the $\bar{p}, \bar{s}, \bar{t}$ and $\bar{d}$ electro-elastic behaviour related to the imperfect parameter with square cell. We denote the material property $d = s/p$ (strain piezoelectric coefficient). The material parameters used in the calculations are the following: $V_2 = 0.5$, $s_2/s_1 = 2$, $t_2/t_1 = 3$ and the matrix is PZT-7A. We point out that the composite properties $\bar{p}$ and $\bar{s}$ become stiffer as χ^* increase for $K \in [100, \infty)$. This trend is the opposite (softer) for $0 < K < 0.01$, where all the curves are indistinguishable for the shear modulus $\bar{p}$; the curves for the piezoelectric modulus $\bar{s}$ are different in this interval. Mahiou and Beakou [29] observed same conclusion for the effective elastic longitudinal shear modulus. The curve for the permittivity effective modulus $\bar{t}$ has the same trend as the elastic effective modulus $\bar{p}$ but they are symmetric with opposite effect. The stress piezoelectric effective coefficient $\bar{d}$ is stiffer for the smallest values of χ^*. Recently, Shodja et al. [42] investigated the effects of different interface conditions on the electro-mechanical response of the matrix-fiber sensor system under loading conditions. Different boundary value problems in a unified manner and various fiber-matrix interface conditions were considered.

7 Conclusions

In the present paper, an asymptotic approach for the simulation of the elastic imperfect bonding in piezo-composite materials is proposed. We introduce a set of elastic springs between the matrix and inclusions that transmits a load from the matrix to the inclusion; the transmission stress is proportional to the displacement jump across the "matrix-inclusion" interface. In the asymptotic limit, we can simulate different degrees of the interface response: the case $K \to \infty$ corresponds to the perfect bonding, the case $K = 0$ to the complete separation of the matrix and inclusions.

As an illustrative example, we consider the axial shear of fiber-reinforced piezoelectric composites with square and hexagonal arrays of cylindrical inclusions. Our analysis is based on the asymptotic homogenization method. The local problems are solved and the solutions are valid for all values of the components volume fractions and properties.

The debonding parameter K can be considered as a kind of phenomenological parameter. Unfortunately, up to now, the authors have not found experimental data related to characterization of the effective coefficients

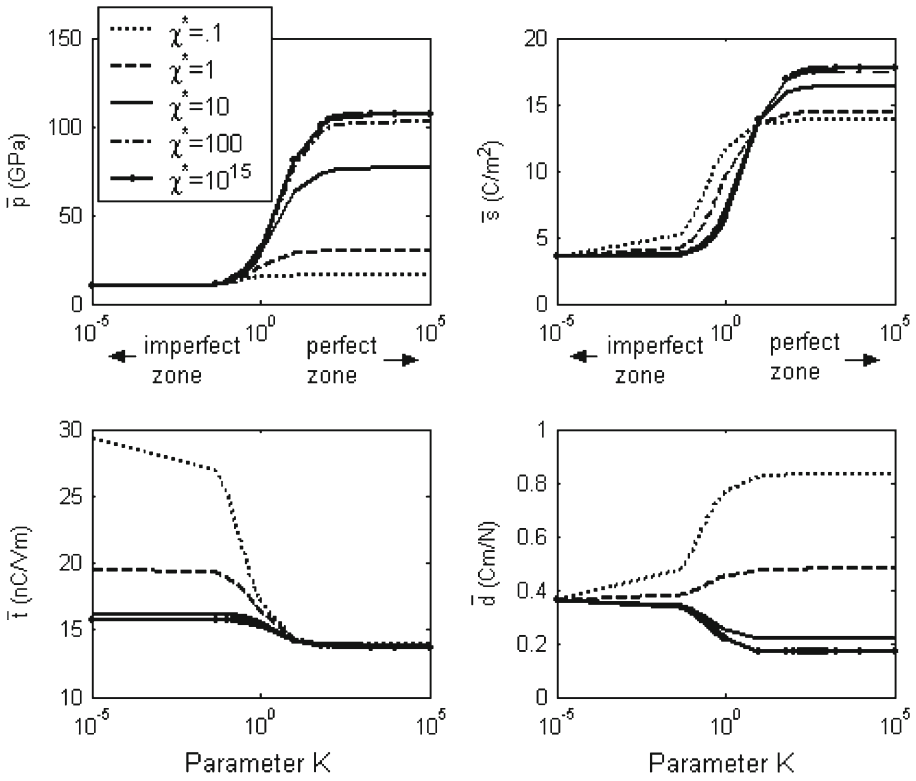

Fig. 4 Electro-elastic effective behavior of $\bar{p}$, $\bar{s}$, $\bar{t}$ and $\bar{d}$ versus imperfect parameter K for different values of elastic shear modulus ratio $\chi^* = p_2/p_1$

in piezoelectric composites under imperfect contact conditions. Evidently, in many practical examples it may not be identified a priori, so the researcher can operate only by some empirical estimations.

Acknowledgments This work was sponsored by CoNACYT project No. 101489. The provisions of the Basic Sciences Program Project CITMA No. 9/2004 and the Department of Basic Science of the Monterrey Institute of Technology, Campus of México State are also acknowledged. Computational support by Ana Pérez Arteaga and Ramiro Chavez is also recognized.

References

1. Andrianov, I.V., Bolshakov, V.I., Danishevs'kyy, V.V., Weichert, D.: Asymptotic simulation of imperfect bonding in periodic fibre-reinforced composite materials under axial shear. Int. J. Mech. Sci. **49**, 1344–1354 (2007)
2. Benveniste, Y.: The effective mechanical behavior of a composite with imperfect contact between the constituents. Mech. Mater. **4**, 197–208 (1985)
3. Benveniste, Y., Miloh, T.: The effective conductivity of composites with imperfect thermal contact at constituent interfaces. Int. J. Eng. Sci. **24**(9), 1537–1552 (1986)
4. Benveniste, Y.: Correspondance relations among equivalent clases of heterogenous piezoelectric solids under anti-plane mechanical and in-plane electric fields. J. Mech. Phys. Solids **43**, 553–571 (1995)
5. Benveniste, Y., Miloh, T.: Imperfect soft and stiff interfaces in two dimensional elasticity. Mech. Mater. **33**, 309–323 (2001)
6. Bövik, P.: On the modelling of thin interface layers in elastic and acoustic scattering problems. Q. J. Mech. Appl. Math. **47**, 17–42 (1994)
7. Bravo Castillero, J., Guinovart Díaz, R., Sabina, F.J., Rodríguez Ramos, R.: Closed-form expressions for the effective coefficients of a fiber-reinforced composite with transversely isotropic constituents-II. Piezoelectric and square symmetry. Mech. Mater. **33**(4), 237–248 (2001)
8. Bruno, O.P.: The effective conductivity of strongly heterogeneous composites. Proc. R. Soc. Lond. A **433**, 353–381 (1991)
9. Dingreville, R., Qu, J., Cherkaoui, M.: Surface free energy and its effect on the elastic behavior of nanosized particles, wires and films. J. Mech. Phys. Solids **53**, 1829–1854 (2005)
10. Duan, H.L., Wang, J., Huang, Z.P., Karihaloo, B.L.: Size-dependent effective elastic constants of solids containing nano-inhomogeneities with interface stress. J. Mech. Phys. Solids **53**, 1574–1596 (2005)
11. Duan, H.L., Karihaloo, B.L.: Thermo-elastic properties of heterogeneous materials with imperfect interfaces: Generalized Levin's formula and Hill's connections. J. Mech. Phys. Solids **55**, 1036–1052 (2007)

12. Goland, M., Reissner, E.: The stresses in cemented joints. J. Appl. Mech. **11**, 17–27 (1944)
13. Guinovart-Díaz, R., Bravo-Castillero, J., Rodríguez-Ramos, R., Sabina, F.J.: Closed-form expressions for the effective coefficients of fibre-reinforced composite with transversely isotropic constituents—I. Elastic and hexagonal symmetry. J. Mech. Phys. Solids **49**, 1445–1462 (2001)
14. Guinovart Díaz, R., Rodríguez Ramos, R., Bravo Castillero, J., Sabina, F.J., Maugin, G.A.: A recursive asymptotic homogenization scheme for multi-phase fibrous elastic composites. Mech. Mater. **37**, 1119–1131 (2005)
15. Guinovart-Díaz, R., Rodriguez-Ramos, R., Bravo-Castillero, J., Sabina, F.J., Maugin, G.A.: Closed-form thermo-elastic moduli of a periodic three-phase fiber-reinforced composite. J. Therm. Stresses **28**, 1067–1093 (2005)
16. Hashin, Z.: Thermoelastic properties of fiber composites with imperfect interface. Mech. Mater. **8**, 333–348 (1990)
17. Hashin, Z.: Thermoelastic properties of particulate composites with imperfect interface. J. Mech. Phys. Solids **39**(6), 745–762 (1991)
18. Hashin, Z.: The spherical inclusion with imperfect interface. J. Appl. Mech. **58**, 444–448 (1991)
19. Hashin, Z.: Thin interphase/imperfect interface in conduction. J. Appl. Phys. **89**, 2261–2267 (2001)
20. Hashin, Z.: Thin interphase/imperfect interface in elasticity with application to coated fiber composites. J. Mech. Phys. Solids **50**, 2509–2537 (2002)
21. Ikeda, T.: Fundamentals of Piezoelectricity. University Press, Oxford (1990)
22. Jasiuk, I., Tong, T.: The effect of interface on the elastic stiffness of composites. Mech. Comput. Mat. Struct. **100**, 49–54 (1989)
23. Jasiuk, I., Kouider, M.W.: The effect of an inhomogeneous interphase on the elastic constants of transversely isotropic composites. Mech. Mater. **15**, 53–63 (1993)
24. Jiang, C.P., Cheung, Y.K.: An exact solution for the three-phase piezoelectric cylinder model under antiplane shear and its applications to piezoelectric composites. Int. J. Solids Struct. **38**, 4777–4796 (2001)
25. Kar-Gupta, R., Venkatesh, T.A.: Electromechanical response of 1–3 piezoelectric composites: Effect of poling characteristics. J. Appl. Phys. **98**, 054102-1/054102-14 (2005)
26. Lipton, R., Vernescu, B.: Composites with imperfect interface. Proc. R. Soc. Lond. A **452**, 329–358 (1996)
27. Lipton, R.: Variational methods, bounds, and size effects for composites with highly conducting interface. J. Mech. Phys. Solids **45**, 361–384 (1997)
28. López-López, E., Sabina, F.J., Bravo-Castillero, J., Guinovart-Díaz, R., Rodríguez-Ramos, R.: Overall electromechanical properties of a binary composite with 622 symmetry constituents. Antiplane shear piezoelectric state. Int. J. Solids Struct. **42**, 5765–5777 (2005)
29. Mahiou, H., Beakou, A.: Modelling of interfacial effects on the mechanical properties of fibre-reinforced composites. Compos. Part A **29A**, 1035–1048 (1998)
30. McPhedran, R.C., McKenzie, D.R.: Electrostatic and optical resonances of arrays of cylinders. Appl. Phys. **23**, 223–235 (1980)
31. Miller, R.E., Shenoy, V.B.: Size-dependent elastic properties of nano-sized structural elements. Nanotechnology **11**, 139–147 (2000)
32. Miloh, T., Benveniste, Y.: On the effective conductivity of composites with ellipsoidal inhomogeneities and highly conducting interfaces. Proc. R. Soc. Lond. A **455**, 2687–2706 (1999)
33. Molkov, V.A., Pobedria, B.E.: Effective elastic properties of a composite with elastic contact. Izvestia Akademia Nauk SSR. Mekhanika Tverdovo Tela. No. 1. 111–117 (1988)
34. Nemat-Nasser, S., Hori, M.: Micromechanics: Overall Properties of Heterogeneous Materials, 2nd revised edn. Elsevier, Amsterdam (1999)
35. Nie, S., Basaran, C.: A micromechanical model for effective elastic properties of particulate composites with imperfect interfacial bonds. Int. J. Solids Struct. **42**, 4179–4191 (2005)
36. Niklasson, A.J., Datta, S., Dunn, M.L.: On ultrasonic guided waves in a thin anisotropic layer lying between two isotropic layers. J. Acoust. Soc. Am. **91**, 1875–1887 (2000)
37. Niklasson, A.J., Datta, S., Dunn, M.L.: On approximating guided waves in plates with thin anisotropic coatings by means of effective boundary conditions. J. Acoust. Soc. Am. **108**, 924–933 (2000)
38. Parton, V.Z., Kudryavtsev, B.A.: Engineering Mechanics of Composite Structures. CRC Press, Boca Raton (1993)
39. Pobedria, B.E.: Mechanics of Composite Materials. Moscow University Press, Moscow (in Russian) (1984)
40. Sabina, F.J, Rodríguez Ramos, R., Bravo Castillero, J., Guinovart Díaz, R.: Closed-form expressions for the effective coefficients of fibre-reinforced composite with transversely isotropic constituents-II: Piezoelectric and hexagonal symmetry. J. Mech. Phys. Solids **49**, 1463–1479 (2001)
41. Sharma, P., Ganti, S., Bhate, N.: Effect of surfaces on the size-dependent elastic state of nanoinhomogeneities. Appl. Phys. Lett. **82**, 535–537 (2003)
42. Shodja, H.M., Tabatabaei, S.M., Kamali, M.T.: A piezoelectric-inhomogeneity system with imperfect interface. Int. J. Eng. Sci. **44**, 291–311 (2006)
43. Torquato, S., Rintoul, M.D.: Effect of the interface on the properties of composite media. Phys. Rev. Let. **75**, 4067–4070 (1995)
44. Wang, J., Duan, H.L., Zhang, Z., Huang, Z.P.: An anti-interpenetration model and connections between intherphase and interface models in particle-reinforced composites. Int. J. Mech. Sci. **47**, 701–718 (2005)